AD-A088 129 VON KARMAN INST FOR FLUID DYNAMICS RHODE-SAINT-GENESE--ETC F/G 16/3
HYPERSONIC WIND TUNNEL STUDY OF A 15 DEG-30 DEG HALF ANGLE CONC--ETC(U)
DEC 79 B E RICHARDS AFOSR-78-3474
UNCLASSIFIED VKI-INTERNAL NOTE-62 AFOSR-TR-80-0629 NL

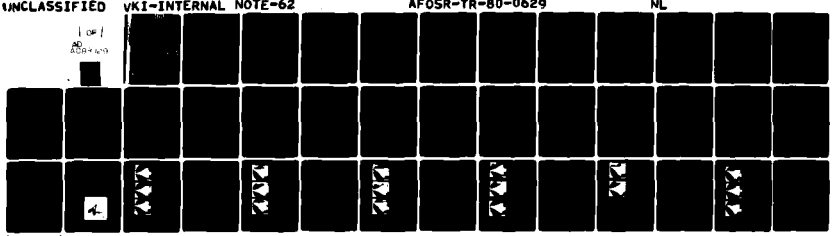

END
DATE FILMED
-80
DTIC

LEVEL II

von KARMAN INSTITUTE

FOR FLUID DYNAMICS

INTERNAL NOTE 62

AFOSR 78-3474

FINAL SCIENTIFIC REPORT
1 DEC 1978 - 30 NOV 1979

HYPERSONIC WIND TUNNEL STUDY OF A 15°-30° HALF ANGLE CONCAVE BICONIC MODEL UP TO HIGH ANGLES OF ATTACK

B.E. RICHARDS

APPROVED FOR PUBLIC RELEASE; DISTRIBUTION UNLIMITED

PREPARED FOR : SAMSO/RSSE
PO BOX 92960
WORLDWAY POSTAL CENTER
LOS ANGELES, CA 90009

AND EOARD
BOX 14
FPO BOX09510

RHODE SAINT GENESE BELGIUM

UNCLASSIFIED

SECURITY CLASSIFICATION OF THIS PAGE (When Data Entered)

REPORT DOCUMENTATION PAGE	READ INSTRUCTIONS BEFORE COMPLETING FORM
1. REPORT NUMBER (19) AFOSR-TR-80-0629	2. GOVT ACCESSION NO. AD-A088729	3. RECIPIENT'S CATALOG NUMBER
4. TITLE (and Subtitle) HYPERSONIC WIND TUNNEL STUDY OF A 15 deg - 30 deg HALF ANGLE CONCAVE BICONIC MODEL UP TO HIGH ANGLES OF ATTACK	5. TYPE OF REPORT & PERIOD COVERED (9) FINAL Rept. 1 Dec 1978 - 30 Nov 1979
	6. PERFORMING ORG. REPORT NUMBER VKI Internal Note 62
7. AUTHOR(s) (10) BRYAN E. RICHARDS (15)	8. CONTRACT OR GRANT NUMBER(s) AFOSR-78-3474
9. PERFORMING ORGANIZATION NAME AND ADDRESS VON KARMAN INSTITUTE CHAUSSEE DE WATERLOO, 72 B-1640 RHODE SAINT GENESE, BELGIUM (16)	10. PROGRAM ELEMENT, PROJECT, TASK AREA & WORK UNIT NUMBERS 2307A1 61102F (17) A1
11. CONTROLLING OFFICE NAME AND ADDRESS AIR FORCE OFFICE OF SCIENTIFIC RESEARCH/NA BLDG 410 BOLLING AIR FORCE BASE, DC 20332 (11)	12. REPORT DATE December 1979
	13. NUMBER OF PAGES 37
14. MONITORING AGENCY NAME & ADDRESS (if different from Controlling Office) VKI-INT. NOTE 62	15. SECURITY CLASS. (of this report) UNCLASSIFIED
	15a. DECLASSIFICATION/DOWNGRADING SCHEDULE

16. DISTRIBUTION STATEMENT (of this Report)

Approved for public release; distribution unlimited

17. DISTRIBUTION STATEMENT (of the abstract entered in Block 20, if different from Report)

18. SUPPLEMENTARY NOTES

19. KEY WORDS (Continue on reverse side if necessary and identify by block number)

HYPERSONIC FLOW
REENTRY
MISSILE
HEAT TRANSFER MEASUREMENTS
PRESSURE MEASUREMENTS
SHOCK BOUNDARY LAYER INTERACTION

20. ABSTRACT (Continue on reverse side if necessary and identify by block number)

Heat transfer and pressure measurements have been measured on a 15^{o} - 30^{o} half angle biconic model with a blunt nosetip in the von Karman Institute Longshot free piston tunnel at Mach 15 and 20 and Reynolds numbers between $1x10^{6}$ and $5x10^{6}$ based on model base diameter. The test flow parameter closely simulated reentry aerodynamic conditions. The angle of attack of the model was varied from 0^{o} to 20^{o}. Information derived from the measurements and also schlieren pictures enabled understanding of the effects of Mach number, Reynolds number and flow incidence on the flow over the model and the location and size of heat transfer peaks.

DD FORM 1 JAN 73 1473 EDITION OF 1 NOV 65 IS OBSOLETE

UNCLASSIFIED

411190

VON KARMAN INSTITUTE FOR FLUID DYNAMICS
AEROSPACE DEPARTMENT
CHAUSSEE DE WATERLOO, 72
B - 1640 RHODE SAINT GENESE, BELGIUM

6

INTERNAL NOTE 62

AFOSR 78-3474

FINAL SCIENTIFIC REPORT

1 DEC 1978 - 30 NOV 1979

HYPERSONIC WIND TUNNEL STUDY OF A 15°-30° HALF ANGLE CONCAVE BICONIC MODEL UP TO HIGH ANGLES OF ATTACK

B.E. RICHARDS

PREPARED FOR :

SAMSO/RSSE
PO BOX 92960
WORLDWAY POSTAL CENTER
LOS ANGELES, CA 90009

AND

EOARD
BOX 14
FPO BOX09510

ARR 7902/BER/LK

ABSTRACT

Heat transfer and pressure measurements have been measured on a 15° - 30° half angle biconic model with a blunt nosetip in the von Karman Institute Longshot free piston tunnel at Mach 15 and 20 and Reynolds numbers between 1 x 10^6 and 5 x 10^6 based on model base diameter. The test flow parameter closely simulated re-entry aerodynamic conditions. The angle of attack of the model was varied from 0 to 20°. Information derived from the measurements and also schlieren pictures enabled understanding of the effects of Mach number, Reynolds number and flow incidence on the flow over the model and the location and size of heat transfer peaks.

TABLE OF CONTENTS

FOREWORD

The activities and results documented in this report were supported under Project 63311F with Captain R. Chambers of Space and Missile Systems Organization, acting as project engineer. This report covers work conducted during the period December 1, 1978 through Noverber 30, 1979.

The technical advice and guidance by Dr Victor DiCristina, Manager, Thermodynamics and Materials Test Department, Avco Systems Division, Wilmington, Mass. in the area of model design and instrumentation was particularly valuable. The author acknowledges the help of Mssrs Roger Conniasselle and Fernand Vandenbroeck in operating the tunnel and Mr Jean-Claude Lobet for the photography. Mr U. Gärtner of the Ruhr-Universität, Bochum, participated in the tests, data reduction and interpretation of the results, while carrying out a "stage" at VKI.

LIST OF FIGURES

LIST OF TABLES

1. INTRODUCTION

In the design of ablation type components for re-entry vehicles, it is critical to be able to predict the flow behaviour on the complicated shapes evoluted during flight. The full problem involves understanding the processes in, for instance, a boundary layer with mass addition from ablation with transition and maybe flow instability present. A useful input can be obtained from the testing of appropriate passive, i.e., non ablating models in flow conditions similar to that expected to be encountered in flight.

Because of lack of advanced facilities in operation at present, and for economic reasons, most parametric test programs are carried out at Mach numbers much below that encountered during the most critical re-entry region with regard to maximum deceleration and maximum surface heating. Studies in the Longshot facility, described in reference 1, have the advantage that mainly exact simulation of Mach number and Reynolds number are achieved with full size models. Hence, using this facility, checks can be made on the lower Mach number studies as well as pinpointing other areas of further necessary study.

Figure 1 demonstrates the families of shapes which have been found on ablating re-entry nosetips. Studies to date have included measurements on 50° - 8° biconic models (representing a "blunt turbulent shape") and hemispheres ("spherical"). The experimental measurements in laminar, transitional, turbulent flow on a variety of smooth and rough-walled models of these types with and without nose bluntness and at various angles of attack, have been compared with appropriate theories (Refs. 2, 3). Pressure and heat transfer measurements have been made on convex shapes (also representing "blunt turbulent" shapes, Ref. 4) and on concave biconic surfaces (representing "transitional" shapes, Ref. 3). Studies of the "unsteady" flow over concave shapes have been made and described in Refs. 5 and 6.

The present series of tests involves a systematic study of the flow over a concave shape which resembles the "sharp turbulent" family of shapes. The study in particular deals with the effect on the flow of Mach number, Reynolds number and model incidence. For the first time in such tests in Longshot the incidence range was extended to 20° reflecting the future interest in the high manoeuvering of missiles within the atmosphere.

2. EXPERIMENTAL APPARATUS AND PROCEDURE

2.1 Test facility

The von Karman Institute Longshot test facility as schematized in figure 2 was used for this program. Longshot differs from a conventional gun tunnel in that a heavy piston is used to compress the nitrogen test gas to very high pressures and temperatures (Refs. 1, 3). The test gas is then trapped in a reservoir at peak conditions by the closing of a system of check valves. The flow conditions decay monotonically during 10 to 20 milli-second running times as the nitrogen trapped in the reservoir flows through the 6° half-angle conical nozzle into the pre-evacuated open jet test chamber. The extremes in supply conditions used in these tests are approximately 55.000 lb/in^2 at 1900°K and 38,000 lb/in^2 at 2320°K. These provide unit Reynolds numbers of 8.5×10^6 and 2×10^6 per ft at nominal Mach numbers of 15 and 20, respectively. The two Mach numbers were obtained at the 14 in. diameter nozzle exit plane by using throat inserts with different diameters.

2.2 Models and instrumentation

The concave conic model designated Model N was supplied by Avco Systems Division and has a 0.375 in nosetip and a 7.28 in. base diameter (see figure 3). The foreward part of the model consisted of a conical section of 15° half angle leading to another conical section of 30° half angle. The transition from these two conical sections was smoothly accomplished through a concave section with a radius of 1.75 in radius from a model radius of 2.10 in. The model was completed with a final uninstrumented section of 6° half angle through a convex section again of radius 1.75 in.

Ten copper calorimeter heat transfer gauges manufactured by BBN and supplied with the models were mounted flush along the surface as illustrated in figure 3. Four were placed on the 15° half angle surface and six placed on the 30° half

angle surface. An additional gauge which was contoured to fit the local shape was placed on the nose of the model. Ten pressure taps were identically spaced along the surface but at 180° around the model from the row of heat transfer gauges. Details of the heat sensors used and the associated recording equipment and data reduction is given in references 7 and 8. The calibration technique used for these transducers is described in reference 4. The gauge calibration factors used for these transducers are given in Table 1. Steady pressure measurements were made using PCB piezo-electric transducers.

The reservoir pressure is measured using Kistler Type 6201 piezo-electric gauges. The reservoir temperature was assessed from signals from a tungsten-rhenium thermocouple mounted in the reservoir. Pitot pressures are measured with a PCB piezo-electric transducer. The tunnel test flow has undergone detailed calibration at the four standard test conditions using fine wire stagnation temperature probes as described in reference 9.

2.3 Schlieren photography

An 18 in conventional single pass Toepler schlieren system equiped with high quality optical components is used. With the exception of one 24 in diameter plane mirror to bend the light 90° (due to the vicinity of a wall near the test section) the light beam takes a Z-shaped path. A single spark light source with a spark duration of 1 usec is used in all tests to record the visualisation of the flow on 3 1/4 x 4 1/4 in. sheet film.

2.4 Test matrix

Table 2 gives the scope of the test series and identifies the test number with each model and flow configuration. It can be seen that the test series provides cross sections of a complete matrix involving the parameters of flow Mach number, Reynolds number and angle of incidence. The test conditions given in this table are nominal values. More detailed information about the test section conditions is given in Table 3.

3. RESULTS AND DISCUSSION

3.1 Presentation of results and general remarks

The overall basic results of the study can be presented in figures 5 - 10. These are displayed in such a way as to facilitate the discussion of the effects of changing various parameters. The schlieren photographs, dimensional heat transfer rate, normalised heat transfer rate and normalised pressure are presented. Figures 5 and 6 present the results for M = 16 and Re = 9 x 10^6 per ft for the angle of attack ranges of $-5° < \alpha < 5°$ and $-20° < \alpha < 20°$ respectively; figure 7, the results for M = 16 and Re = 4.5 x 10^6 per ft for $-20° < \alpha < 20°$; Figures 8 and 9 present the results for M = 20 and Re/ft = 3.3 x 10^6 for $-5° < \alpha < 5°$ and $-20° < \alpha < 20°$ respectively and figure 10 presents the results for M = 20 and Re/ft of 2 x 10^6 for $-20° < \alpha < 20°$.

The experimental and normalised results for all tests are also presented in Tables 4 - 7. The pressures are normalised with respect to the pitot pressure, which is assumed to be the same as the stagnation point pressure. The heat transfer rates are normalised with respect to the theoretical stagnation point heat transfer on a 0.375 in radius hemisphere, whose value is given in Table 3 and which is calculated from free stream conditions using the Fay and Riddell formula as presented in reference 7.

A negative incidence, α, in the figures represents a "leeward" surface, and a positive value a "windward" surface. Since during one particular test the heat transfer gauges are on a windward surface when the pressure taps are on the leeward surface and vice versa, the figures are rearranged to align data on surfaces with the same attitude to the flow rather than in terms of run numbers (as in the case of the tabulated data).

3.2 Discussion

3.2.1 Pressure measurements

The pressure measurements were non-dimensionalised with respect to the measured pitot pressure and plotted against the distance from the nose along the surface of the model. In order to assist discussion of the results, then simple Newtonian and tangent cone theories were plotted, where possible, on the graphs.

For the majority of windward flow cases the information from both the schlieren pictures and the pressure distributions indicate that little or no separation is occuring at the junction between the forebody and the aft body. In these cases the pressure distribution is characterised by a flat distribution of the four pressures before the corner, followed by a marked peak on the fifth gauge and a decrease to a fairly flat distribution on the last three or four gauges. The pressure peak is caused essentially by the change in momentum of the flow as it is turned rapidly through the corner. Newtonian theory agrees best with the forebody results, but after the peak, both Newtonian theory and tangent cone theory overpredict the results.

It is evident for the zero angle of attack cases, that since the pressure peak moves to the fifth (or even the sixth gauge for the low Reynolds number cases) that the flow has become separated, and that the separation length is increasing with Reynolds number, a feature of transitional flow.

For the "leeward" flow cases at 5°, the flow is evidently highly separated with the re-attachment point moving towards the model shoulder, and again the separation length is increasing with decreasing Reynolds number. At 20°, the flow is difficult to diagnose since schlieren pictures show little viscous flow detail but the pressures tend to show characteristics of unseparated flow. Furthermore the measurements have very low values and are very scattered.

3.2.2 Heat transfer measurements

For these measurements, no suitable computer code was available at the Institute for prediction of these flows which has complicated the diagnosis of the flow. The discussion is broken down into the behaviour at different surface incidences.

3.2.2.1 Zero angle of attack

The heat transfer distributions here are characterised by very high peak heating at re-attachment of the separated boundary layer at values sometimes 20 times that on the forebody. Since the gauges are widely spaced, then the re-attachment point may fall between gauges resulting in lower heat transfer rates than otherwise. For the high Reynolds number cases, the heat transfer rate on the after body after separation is at a higher level than for low Re cases indicating transition to turbulent flow.

3.2.2.2 5° angle of attack, wind-ward surfaces

Within the scatter of the measurement, the heat transfer rate appears to increase uniformly by two to three times as one goes from the forebody to the after body, again providing evidence that the flow is unseparated. The schlieren picture shows that the flow is probably turbulent on the aft body for the high Reynolds number case ($M = 16$, $Re = 9 \times 10^6$).

3.2.2.3 5° angle of attack, "leeward" surfaces

For both of the cases examined, the peak heating occurs at the seventh gauge, indicating that the re-attachment point of the undoubtably separated flow lies near this point. There is a difference however in the distribution of heat transfer before the peak. In the high Reynolds number case the heat transfer rate is increasing with distance, typical of a transitional or turbulent separator, whilst for the low Reynolds case there occurs a "bucket" indication of a laminar separation.

3.2.2.4 20° angle of attack, windward surface

The distributions illustrated here are very difficult to recreate with known flow behaviour. It is established from schlieren photographs and pressure disturbances that the flow on the windward meridian is attached. Nevertheless the flow is unusual because of the high angle exposed to the flow and the high depletion of the flow by the strong cross flow likely to exist. The most common feature in the results is that there occurs a peak at the eighth gauge. At the highest Reynolds number case, there occurs another peak of almost equivalent size to the latter peak occuring at about the third gauge and which diminishes in size with decreasing Reynolds number. Transition may play a role in this unusual feature. Furthermore detailed research is suggested to understand these results.

3.2.2.5 20° angle of attack, leeward surface

In these cases, the forebody is at a negative angle of incidence to the flow, and the flow boundary layer would be thickening due to the cross flow. The heat transfer rates are typically one order of magnitude smaller than on the windward surface and the results are highly scattered. Nevertheless the impression gained from the result is that of an unseparated flow characteristic with a peak heat transfer found at the fifth gauge i.e. the one after the corner.

4. CONCLUSIONS

Pressure and heat transfer measurements and visualization of the flow were made on a 15°-30° biconic concave shape with a spherical nose tip representing the sharp turbulent configuration in the family of body shapes found during reentry ablation. The measurements were made in the flow of the von Karman Institute Longshot Facility at nominal Mach numbers of 16 and 20 and Reynolds numbers of 9.0×10^6, and 4.5×10^6, 3.0×10^6 and 2.0×10^6, respectively. The effect of changing the incidence over a range from -20° to +20° was studied.

Generally Newtonian theory predicted well pressures under attached flows on the forebody but overpredicted measurements on the aft body, as also did tangent cone theory. The measurements ascertained that on windward surfaces the flow remained attached to the surface, but in all other cases flow separation occurred. However, there were signs that for the leeward surface of the cone at 20° incidence the flow also remained attached. As expected, heat transfer rates near reattachment exceeded by up to 20 times those occurring before separation. Trends indicate that the separated regions increased with decreasing Reynolds number, a sign of the existence of transitional flow.

The measurements were generally easy to explain with existing knowledge, except for the case of the strange heat transfer distributions measured on the windward side of the model when it was placed at 20° angle of attack.

REFERENCES

1. RICHARDS, B.E. & ENKENHUS, K.R.: Hypersonic testing in the VKI Longshot piston tunnel.
AIAA J. Vol. 8, No. 6, June 1970, pp 1020-1025.

2. RICHARDS, B.E.; DiCRISTINA, V,; MINGES, M.L.: Heat transfer and pressure distribution on sharp and finite bluntness biconic and hemispherical geometries at various angles of attack in a Mach 15-20 flow.
Astronautical Research 1971; ed. L.G. Napolitano;
D. Reidel Publ. Co., Dordrecht, Holland, 1973, pp 91-103.

3. DiCRISTINA, V. & RICHARDS, B.E: Heat transfer studies on ablation protected nosetips at re-entry simulated conditions.
AIAA P 77-781; 12th Thermophysics Conf. Albuquerque, New Mexico, June 1977.

4. RICHARDS, B.E.: Experimental study of the hypersonic flow over a convex conic model resembling the nosetip of a re-entry vehicle.
VKI IN 59, Scientific Report for USAF Grant AFOSR 76-2942, February 1978.

5. KENWORTHY, M.A. & RICHARDS, B.E.: A study of the unsteady flow over concave conic model at Mach 15 and 20.
AFML TR 75-138, September 1975.

6. RICHARDS, B.E.: Heat transfer and pressure measurements on a concave conic model under both steady and unsteady flow conditions.
VKI IN 61, Scientific Report for USAF Grant AFOSR 78-3474, January 1979.

7. RICHARDS, B.E.; CULOTTA, S.; SLECHTEN, J.: Heat transfer and pressure distributions on re-entry nose shapes in the VKI Longshot hypersonic tunnel.
AFML TR 71-200, June 1971.

8. RICHARDS, B.E.: Developments in heat transfer measurements using transient techniques.
ICIASF' 77 Record. Proc. 7th Int. Congress on Instrumentation in Aerospace Simulation Facilities;
Shrivenham, UK; IEEE Publication 77 CH 1251-8 AES;
September 1977, pp 81-88.

9. BACKX, E. & RICHARDS, B.E.: Measurement of stagnation temperatures of 2500 K in a hypersonic flow of 10 msec duration using a fine wire probe.
ICIASF' 77 Record. Proc. 7th Int. Congress on Instrumentation in Aerospace Simulation Facilities;
Shrivenham, UK; IEE Publication 77 CH 1251-8 AES,
September 1977, pp 95-100.

TABLE 1 HEAT SENSOR CALIBRATION INFORMATION

POSITION NO	GAUGE NO	RUNS USED	CALIBRATION CONSTANT $\frac{B.Th.U/ft^2sec}{mV/sec}$
0	23	609	0.625
	24	612-614	0.677
	21	615	0.669
1	1	609-624	0.624
2	3	609-624	0.628
3	5	609-624	0.607
4	6	609-624	0.658
5	7	609-620	0.609
	15A	621-624	0.612
6	9	609-614	0.654
	15	615-616	0.820
	9A	617-620	0.796
	18A	621-624	0.585
7	10	609-624	0.689
8	12	609-624	0.590
9	14	609-624	0.636
10	16	609-624	0.598

TABLE 2 TEST IDENTIFICATION - MODEL N

INCIDENCE / TEST CONDITIONS	0	+5†	-5	+20	-20
M = 16 * Re = 9×10^6/ft	612°	613	614	620	621
M = 16 Re = 5×10^6/ft	611	-	-	619	622
M = 20 Re = 3×10^6	610	616	615	617	623
M = 20 Re = 2×10^6	609	-	-	618	624

KEY

° Test number

* Nominal test section conditions

† Positive incidence means pressure surface "windward"

TABLE 3 TEST CONDITIONS

	T(MS)	PO(PSI)	TO(K)	P1TOT(PSI)
	MACH NO	POP(PSI)	TO P(K)	RE/FT
	P(PSI)	T(K)	RHO	V(FT/SEC)
	QD(LB/FT××2)	Q(BTU)	TT2R(K)	CONDENSATION
1.	0.000	0.550000E 05	0.190000E 04	0.200000E 02
	15.990	0.798927E 05	0.245702E 04	0.872964E 07
	0.780727E-01	0.471264E 02	0.746250E-04	0.734354E 04
	0.201217E 04	0.939885E 02	0.219290E 04	0.432018E 02
2.	0.000	0.350000E 05	0.202000E 04	0.150999E 02
	15.470	0.394981E 05	0.247216E 04	0.465051E 07
	0.484203E-01	0.505899E 02	0.431134E-04	0.736132E 04
	0.116814E 04	0.721548E 02	0.220516E 04	0.408538E 02
3.	0.000	0.590000E 05	0.235000E 04	0.800000E 01
	19.906	0.716570E 05	0.303404E 04	0.313777E 07
	0.154730E-01	0.378117E 02	0.184330E-04	0.818913E 04
	0.618078E 03	0.668823E 02	0.265925E 04	0.368548E 02
4.	0.000	0.376000E 05	0.232000E 04	0.519999E 01
	19.178	0.388046E 05	0.286190E 04	0.206365E 07
	0.108387E-01	0.383805E 02	0.127209E-04	0.794881E 04
	0.401877E 03	0.503513E 02	0.252000E 04	0.354101E 02

Case 1, M_{nom} = 15, High Re.

Case 2, M_{nom} = 15, Low Re.

Case 3, M_{nom} = 20, High Re.

Case 4, M_{nom} = 20, Low Re.

TABLE 4 HEAT TRANSFER MEASUREMENTS

M	Re×10^{-6} (ft^{-1})	Incid.† (deg.)	Run N°		Gauge 1	2	3	4	5	6	7	8	9	10
16	9	0	612	-	17.1	9.4	9.8	5.0	40.3	115.8	60.6	-	68.0	72.9
		+5	614	-	22.7	23.5	21.9	21.0	107.7	78	129.7	114.3	61.9	80.7
		-5	613	-	7.9	7.1	5.6	0	12.9	25.6	57.4	93.1	48.0	45.7
		+20	621	-	116.8	105.7	155.5	137.4	101.6	70.9	167.5	190.8	140.7	126.2
		-20	620	-	3.34	3.31	4.10	4.86	16.7	9.1	6.6	5.2	3.2	4.7
15	4.5	0	611	-	10.6	13.7	6.5	6.4	20.4	78.6	54.6	65.9	51.8	58.5
		+20	622	-	55.4	49.4	69.1	76.0	66.3	59.4	107.7	124.9	94.7	79.2
		-20	619	-	2.69	2.31	3.90	5.30	17.2	7.9	5.5	4.7	4.2	6.7
20	3.3	0	610	147	10.8	8.3	4.4	4.1	10	36.8	135.9	41.3	45.4	32.5
		+5	615	257	41.0	33.7	43.2	36.3	95.6	64.2	60.2	82.5	75.8	73.1
		-5	616	-	23.4	22.7	14.2	11.8	-	21.0	48.8	72.9	54.2	56.8
		+20	623	-	62.1	58.1	58.0	33.9	51.9	36.6	76.0	91.0	64.8	58.3
		-20	617	-	2.7	2.5	3.1	3.8	11.2	8.7	7.0	10.0	6.1	8.5
20	2.0	0	609	-	9.3	8.7	4.0	2.9	7.3	12.9	29.0	18.6	21.8	19.9
		+20	624	-	43.7	41.3	37.5	29.3	36.6	27.3	60.7	90.0	41.9	43.4
		-20	618	-	1.72	1.31	1.44	1.45	9.86	4.24	4.81	4.51	3.44	4.0

† Positive incidence means relevant surface "windward"

TABLE 5 NON-DIMENSIONALISED* HEAT TRANSFER MEASUREMENT

M	Rex10^{-6} (ft^{-1})	Incid^{+} (deg)	Run N°	Theoretical Stag pt heating	Gauge 1	2	3	4	5	6	7	8	9	10
16	9	0	612	300	0.057	0.031	0.033	0.017	0.134	0.386	0.202		0.227	0.243
		+5	614		0.075	0.078	0.073	0.070	0.359	0.26	0.432	0.381	0.206	0.269
		-5	613		0.026	0.024	0.019	0	0.043	0.085	0.191	0.310	0.016	0.152
		+20	621		0.389	0.352	0.518	0.458	0.338	0.236	0.558	0.636	0.469	0.421
		-20	620		0.011	0.011	0.014	0.016	0.056	0.030	0.022	0.017	0.011	0.016
15	4.5	0	611	226	0.047	0.061	0.029	0.028	0.090	0.348	0.242	0.292	0.229	0.259
		+20	622		0.245	0.218	0.306	0.336	0.293	0.262	0.476	0.552	0.419	0.350
		-20	619		0.012	0.010	0.017	0.023	0.076	0.035	0.024	0.021	0.019	0.030
20	3.3	0	610	205	0.053	0.04[illegible]	0.021	0.02	0.005	0.180	0.662	0.201	0.221	0.158
		+5	615		0.200	0.164	0.211	0.177	0.466	0.313	0.294	0.402	0.370	0.357
		-5	616		0.114	0.111	0.069	0.058	-	0.102	0.238	0.356	0.264	0.277
		+20	623		0.303	0.283	0.283	0.165	0.253	0.178	0.370	0.443	0.316	0.284
		-20	617		0.013	0.012	0.015	0.019	0.055	0.042	0.034	0.049	0.030	0.041
20	2.0	0	609	174	0.053	0.050	0.023	0.017	0.042	0.074	0.167	0.107	0.125	0.114
		+20	624		0.251	0.237	0.215	0.168	0.210	0.157	0.349	0.517	0.241	0.249
		-20	618		0.010	0.007	0.008	0.008	0.057	0.024	0.028	0.026	0.020	0.023

* With respect to the theoretical stagnation point heat transfer on a 0.375 in shhere

TABLE 6 PRESSURES LB/IN^2

M	Rex10^{-6} (ft^{-1})	Incid† (deg)	Run N°	Pitot pressure	Gauge 1	2	3	4	5	6	7	8	9
16	9	0	612	31.4	1.39	1.31	1.22	1.72	4.45	13.5	6.23	6.11	6.30
		+5	613	29.6	2.16	2.29	2.51	2.95	14.8	10.3	8.6	8.3	12.5
		-5	614	30.2	1.03	0.91	0.75-0.98	1.05	1.25	2.31	4.91	7.26	5.32
		+20	620	27.8	8.56	8.84	9.09	8.36	21.5	15.1	13.6	13.7	13.4
		-20	621	30.0	0.41-0.47	0.53	0.35	0.38	0.89	0.74	0.54	0.48	
15	4.5	0	611	16.9	0.96	0.62	0.86	1.48	2.38	6.61	2.95	3.86	4.67
		+20	619	16.2	5.28	5.66	5.57	5.28	14.3	10.34	9.19	9.32	10.6
		-20	622	15.9	0.26-0.32	0.33	0.22	0.25	0.55	0.47	0.43	0.30	
20	3.3	0	610	7.2	0.49	0.47	0.76	0.80	0.96	2.91	2.88	1.65	2.18
		+5	616	8.30	0.82	0.76	0.88	0.62-0.75	5.1-5.4	2.6-3.0	2.65	2.54	3.04
		-5	615	7.71	0.38	0.33-0.43	0.52-0.64	0.63	0.76	1.08	1.28	1.65	1.8-3.0
		+20	617	7.7	2.82	2.95	2.88	2.73	6.73	4.65	4.22	4.31	4.8-9.9
		-20	623	7.32	0.17-0.25	0.19-0.21	0.14-0.18	0.13-0.15	0.26	0.20	0.17	0.17	
20	2.0	0	609	5.44	0.34	0.30-0.49	0.54	0.56	0.63	1.57	2.05	1.38-1.83	1.34
		+20	618	4.88	2.00	1.68-2.10	2.01-1.73	1.96	4.78	3.10-3.32	3.10-3.34	3.10-3.39	6.93
		-20	624	4.88	-0.110	0.118-0.131	0.093-0.105	0.083-0.10	0.160	0.135	0.138	0.122	

† Positive incidence means revelant surface "windward"

TABLE 7 NON-DIMENSIONAL PRESSURES

M	Rex10^{-6} (ft^{-1})	Incid† (deg)	Run N°	Gauge 1	2	3	4	5	6	7	8	9
16	9	0	612	0.044	0.042	0.039	0.055	0.142	0.430	0.198	0.195	0.200
		+5	613	0.073	0.077	0.085	0.099	0.5	0.348	0.290	0.280	
		-5	614	0.034	0.030	0.025-0.035	0.035	0.041	0.076	0.162	0.240	0.176
		+20	620	0.308	0.318	0.327	0.301	0.773	0.543	0.489	0.492	0.482
		-20	621	0.015	0.018	0.012	0.013	0.030	0.025	0.018	0.016	
15	4.5	0	611	0.057	0.037	0.051	0.088	0.141	0.391	0.175	0.228	0.276
		+20	619	0.326	0.350	0.344	0.326	0.882	0.638	0.567	0.575	0.654
		-20	622	0.016-0.020	0.020	0.014	0.016	0.035	0.030	0.027	0.019	
20	3.3	0	610	0.068	0.065	0.106	0.111	0.133	0.404	0.40	0.229	0.302
		+5	616	0.099	0.091	0.106	0.074-0.090	0.614-0.651	0.313-0.361	0.319	0.306	0.366
		-5	615	0.049	0.043-0.056	0.067-0.083	0.082	0.098	0.140	0.166	0.214	0.23
		+20	617	0.365	0.383	0.373	0.354	0.873	0.603	0.547	0.558	0.62
		-20	623	0.023-0.034	0.026-0.029	0.019-0.024	0.018-0.02	0.036	0.027	0.023	0.023	
20	2.0	0	509	0.0625	0.055-0.09	0.099	1.03	0.116	0.289	0.377	0.253-0.336	0.246
		+20	618	0.041	0.34-0.43	0.41-0.35	0.401	0.978	0.635-0.680	0.635-0.684	0.635-0.695	
		-20	624	0.022	0.024-0.027	0.019-0.0215	0.017-0.020	0.033	0.028	0.028	0.025	

† Positive incidence means relevant surface "windward"

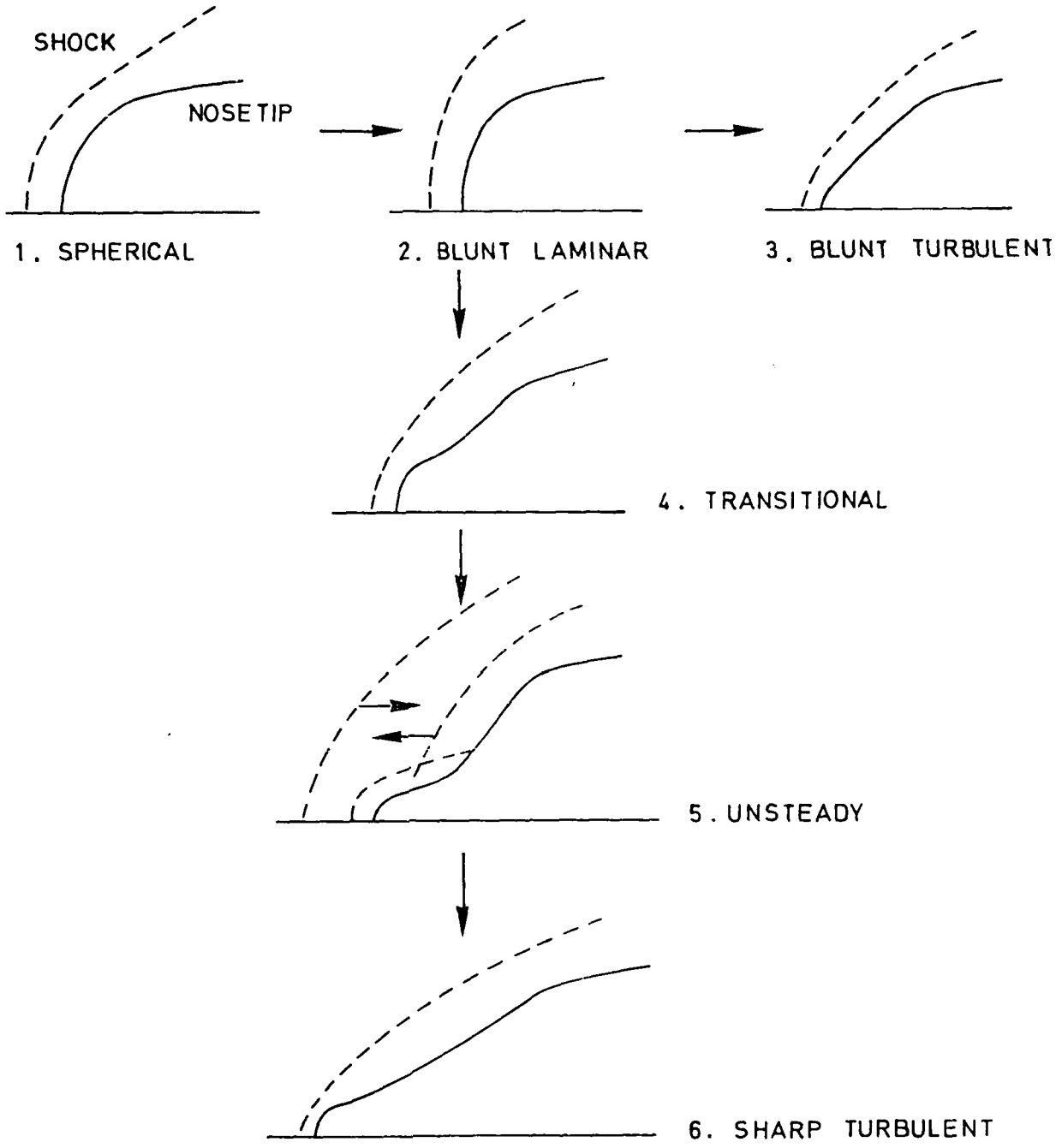

FIG. 1 - NOSETIP SHAPE EVOLUTION

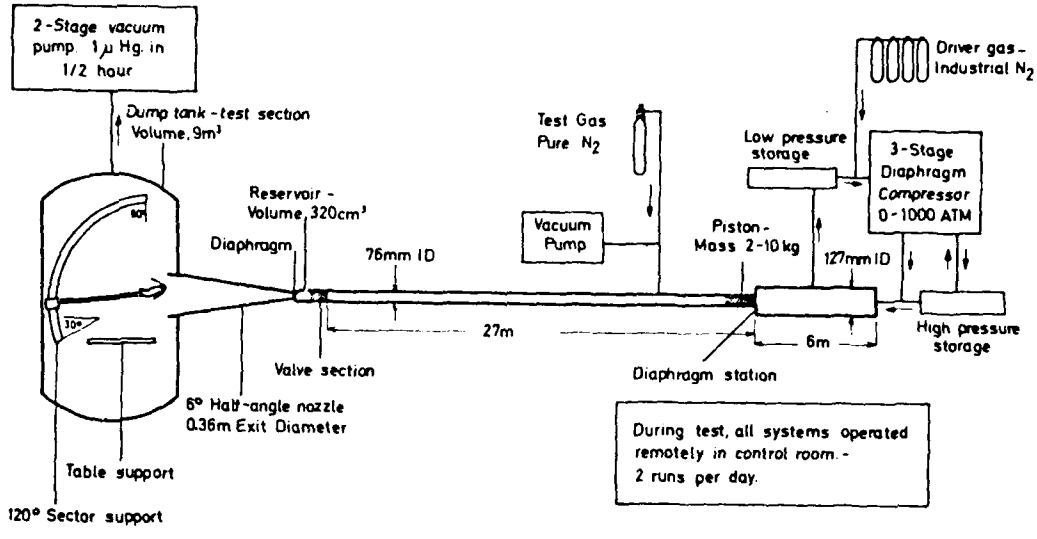

FIG. 2 SCHEMATIC OF THE LONGSHOT FREE PISTON TUNNEL

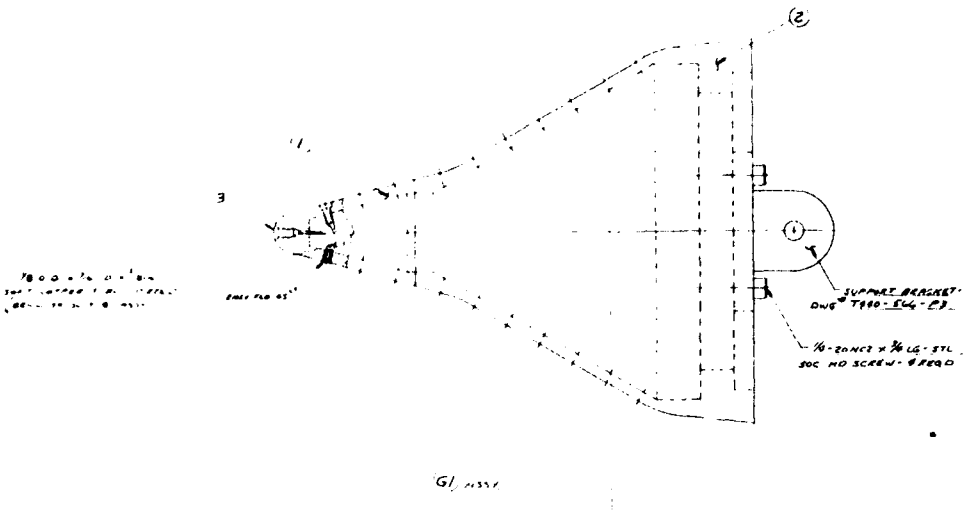

FIG. 3 - SCHEMATIC OF MODEL N

FIG. 4 - PHOTOGRAPH OF MODEL N

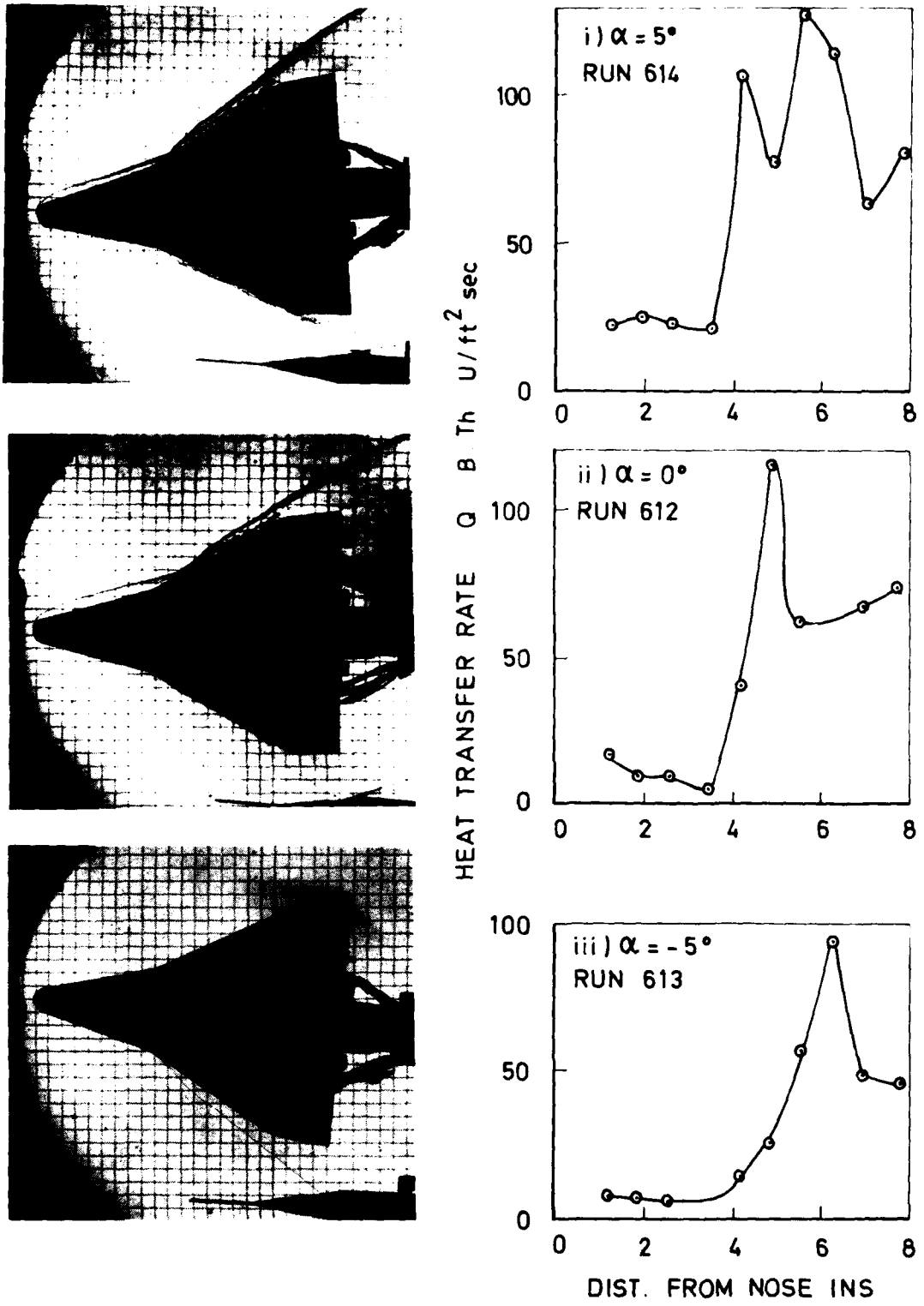

FIG. 5a -SCHLIEREN PHOTOGRAPHS AND HEAT TRANSFER RATE

M = 16, Re = 9×10^6 per ft $-5° < \alpha < 5°$

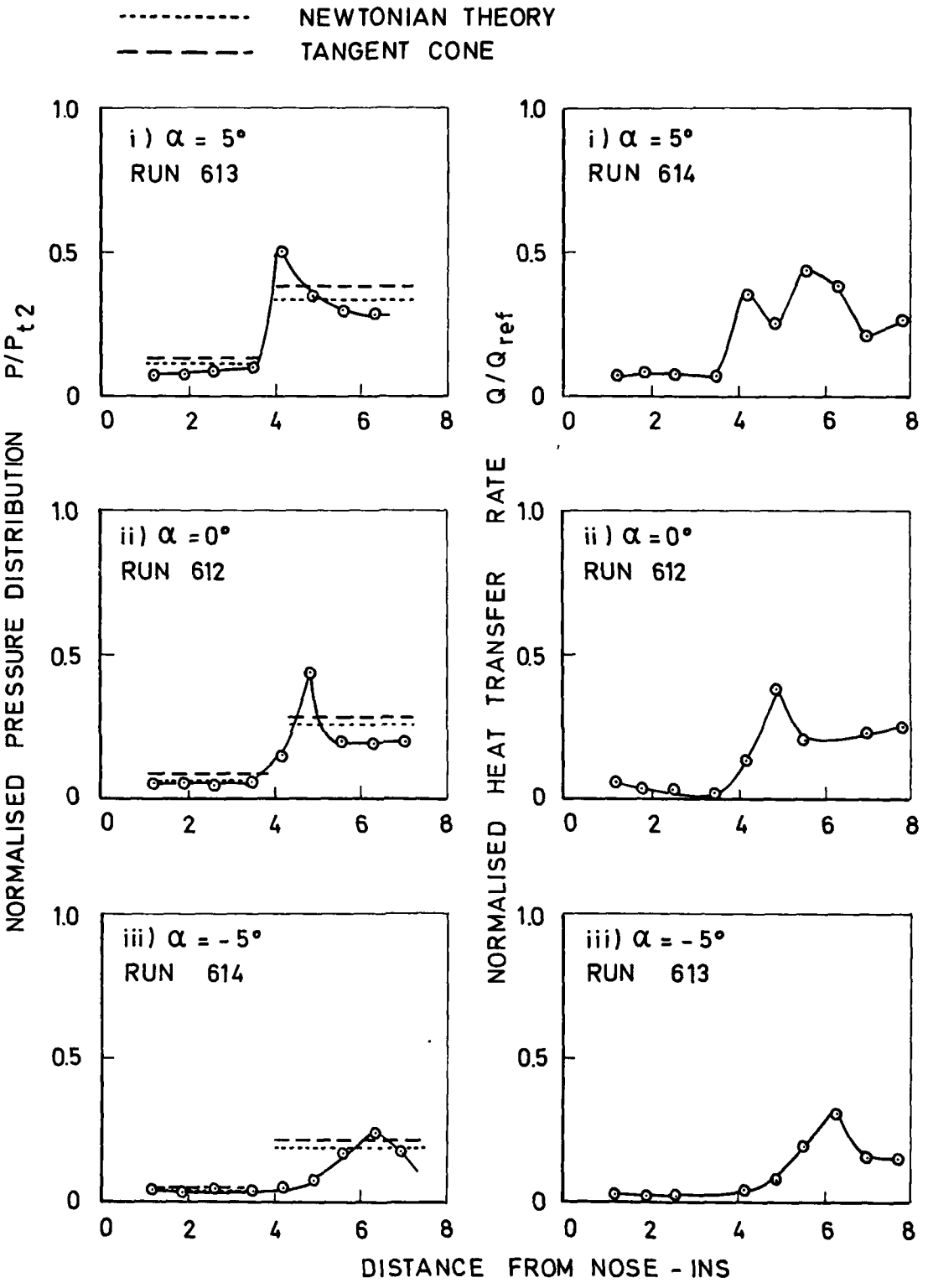

FIG. 5 b - NORMALISED PRESSURE AND HEAT TRANSFER DISTRIBUTIONS

$M = 16 \quad Re = 9 \times 10^6$ per ft. $-5° < \alpha < 5°$

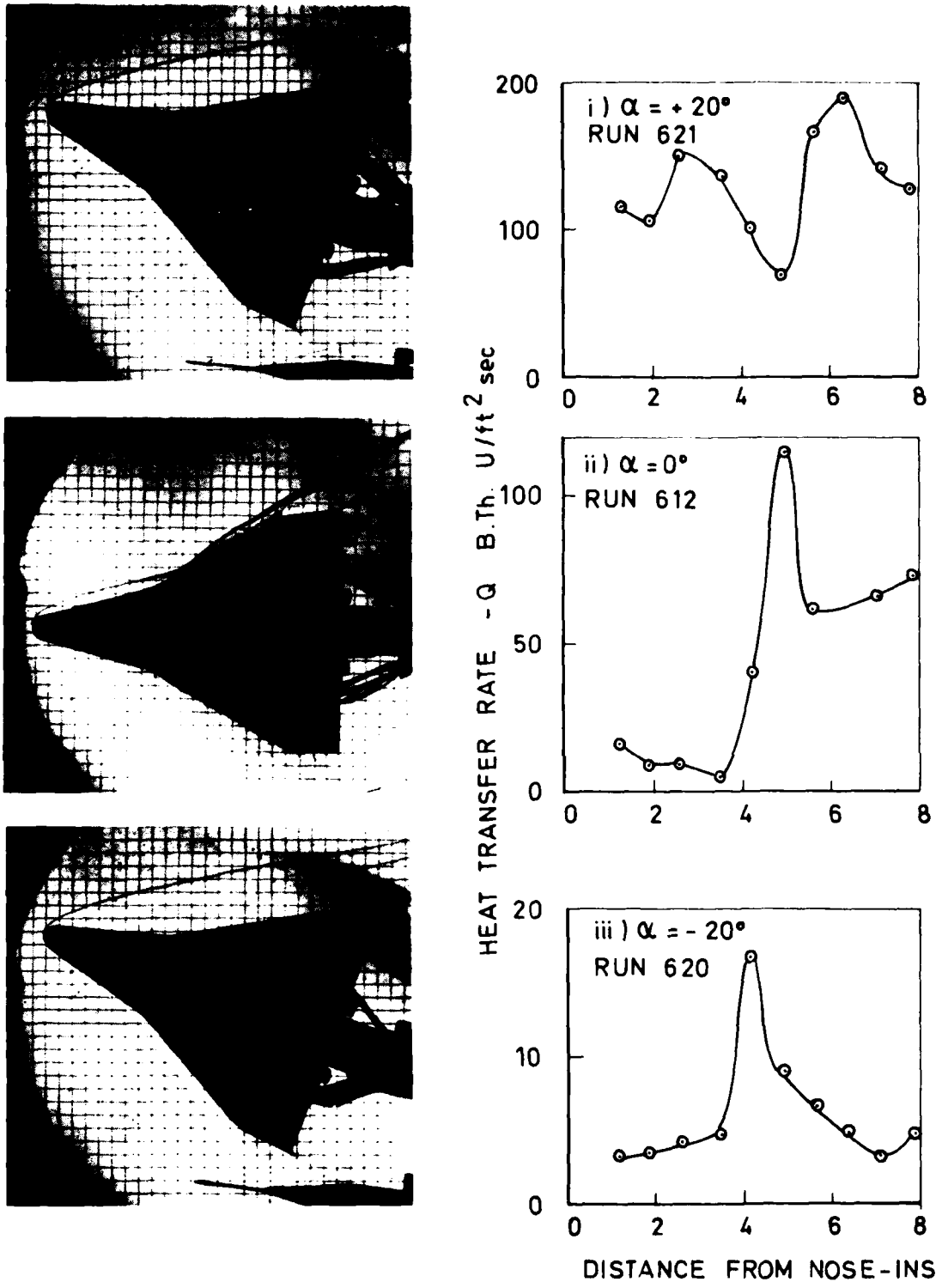

FIG. 6a SCHLIEREN PHOTOGRAPHS AND HEAT TRANSFER RATE

M = 16 $Re = 9 \times 10^6$ $-20° < 0 < 20°$

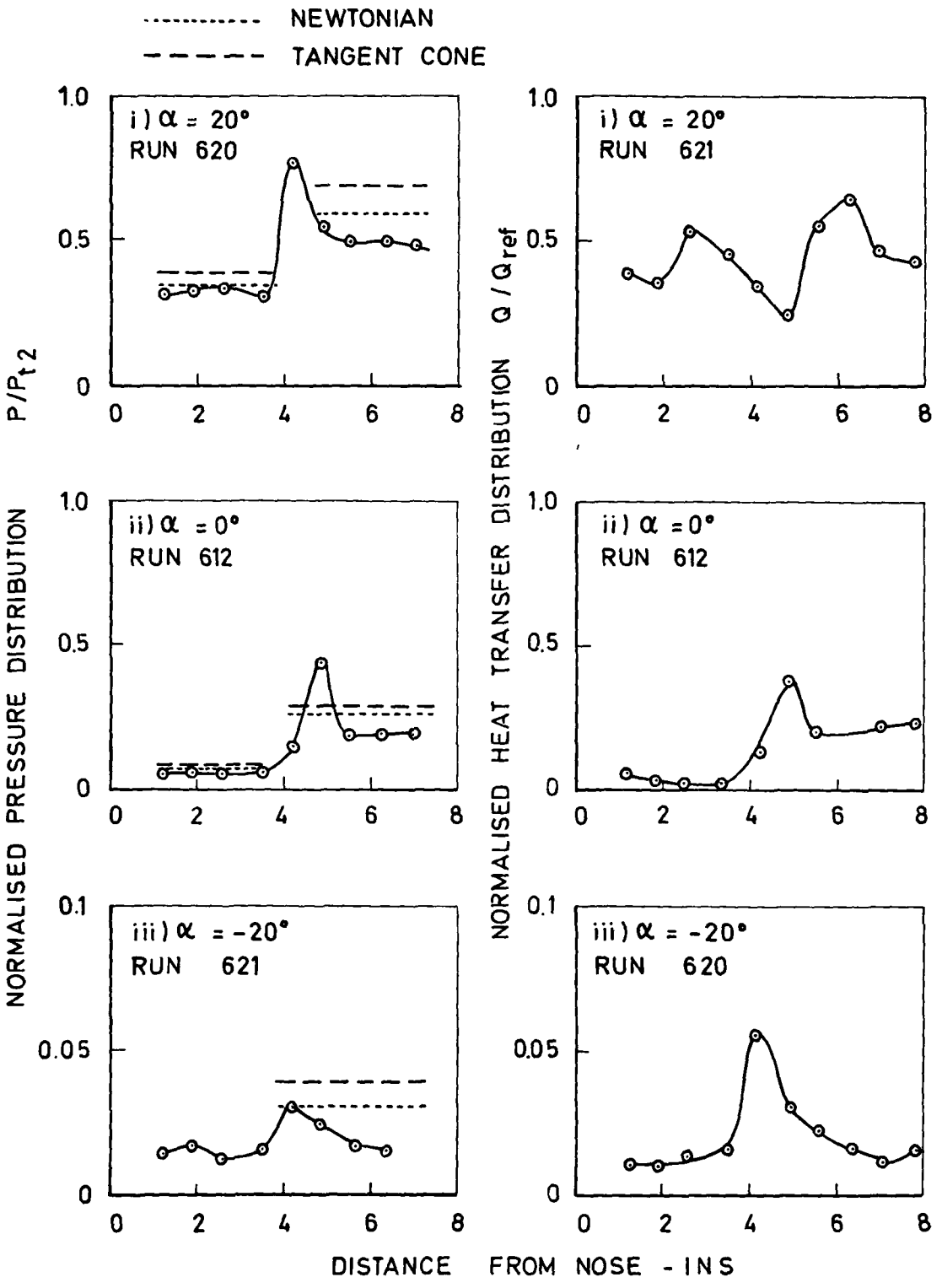

FIG. 6 b - NORMALISED PRESSURE AND HEAT TRANSFER DISTRIBUTION.
M = 16 Re = 9×10^6 per ft. $-20° < \alpha < 20°$

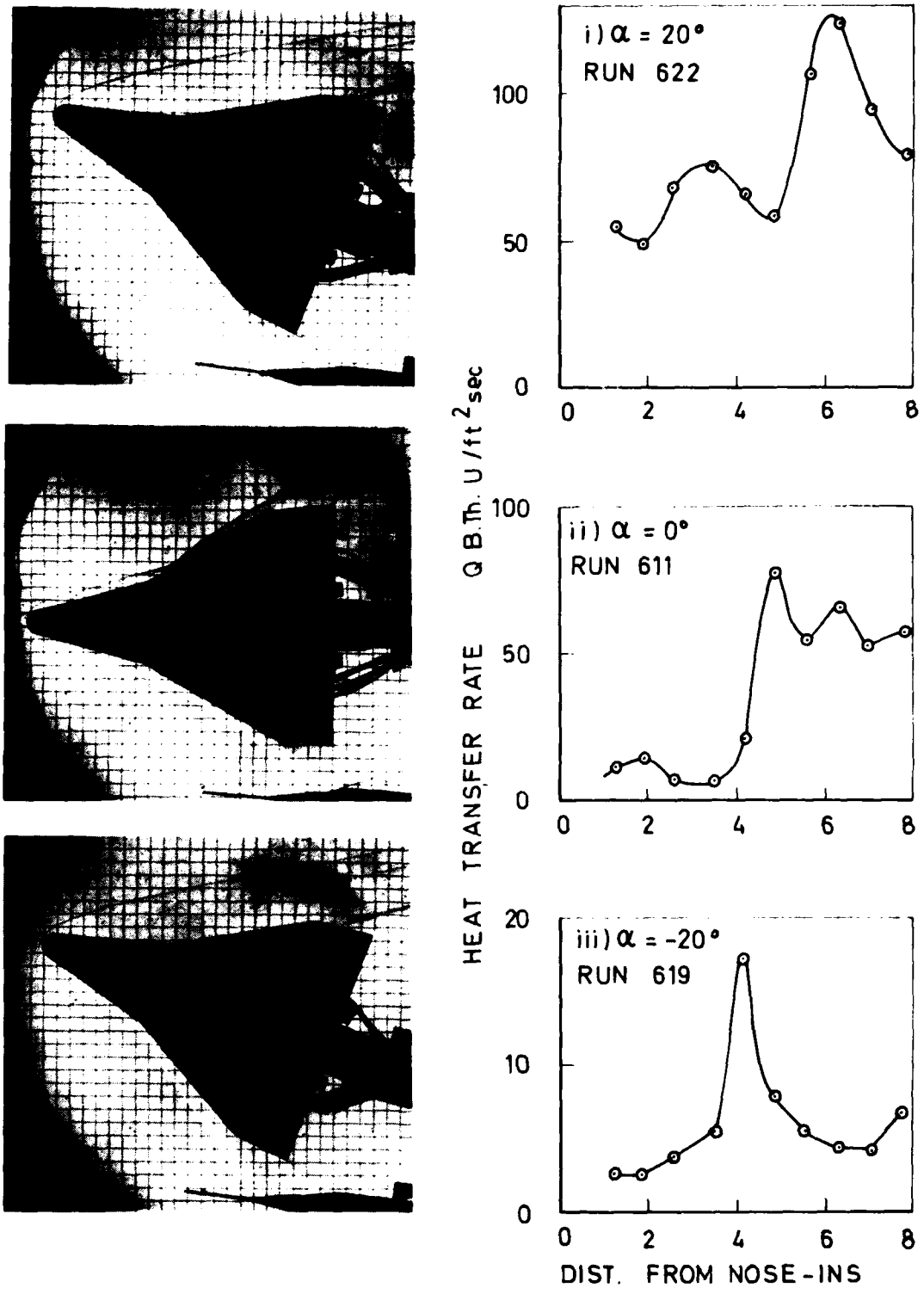

FIG 7a SCHLIEREN PHOTOGRAPHS AND HEAT TRANSFER RATE

M = 15 Re = 4.5×10^6 per ft $20° < \alpha < 20°$

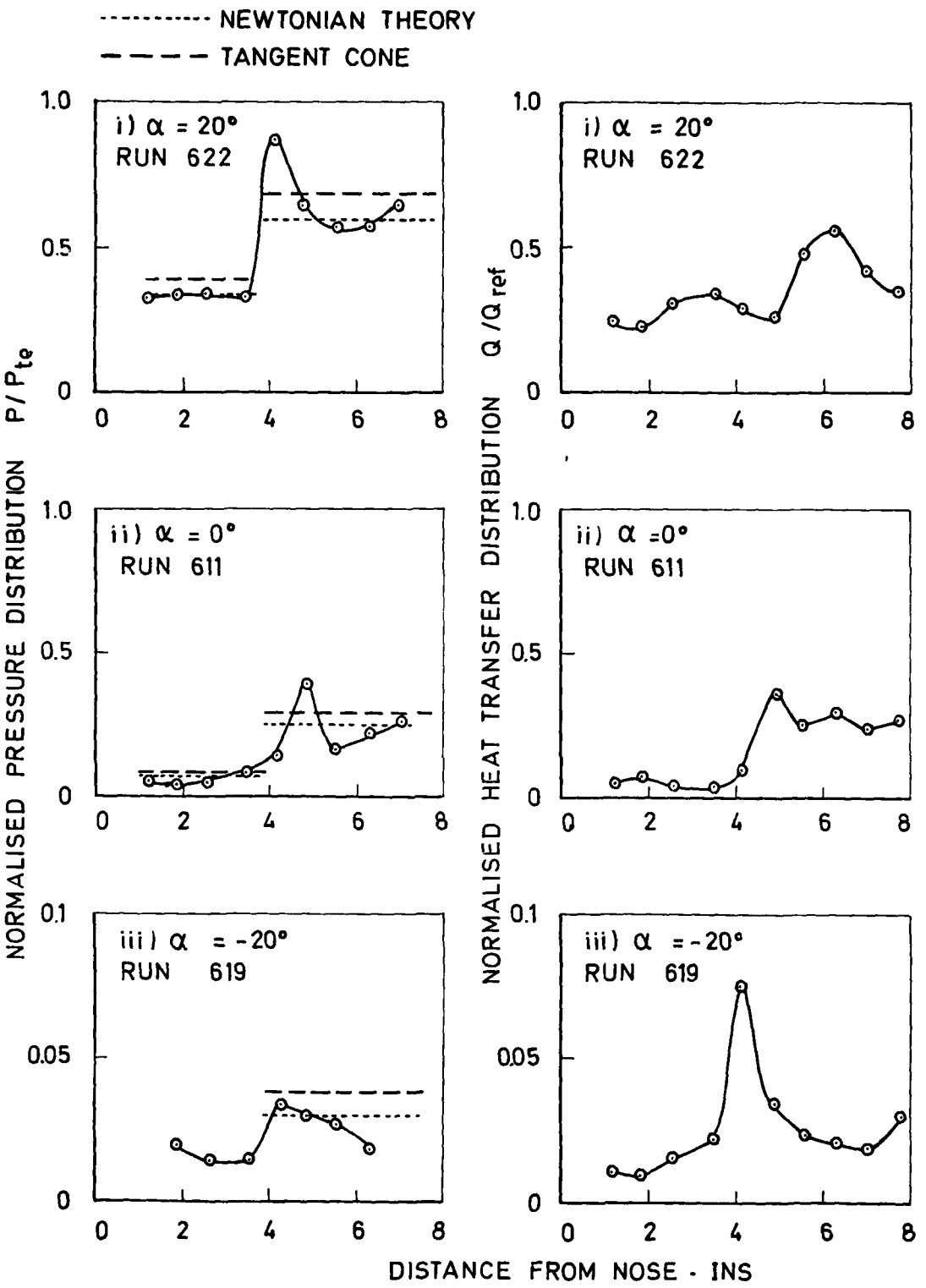

FIG. 7b - NORMALISED PRESSURE AND HEAT TRANSFER DISTRIBUTION.

M = 15 Re = 4.5×10^6 per ft. $-20° < \alpha < 20°$

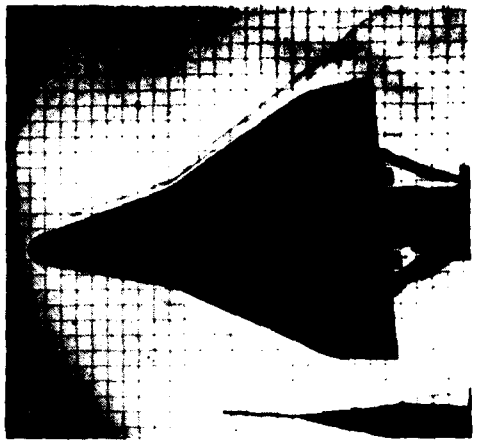

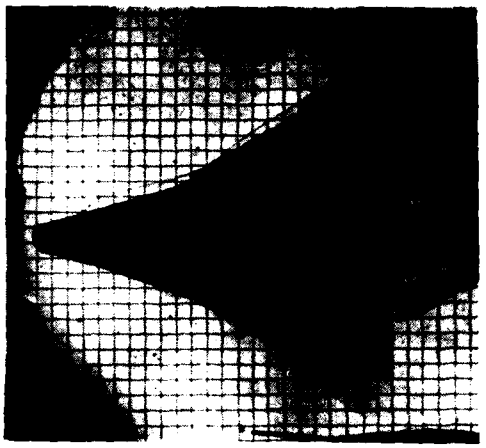

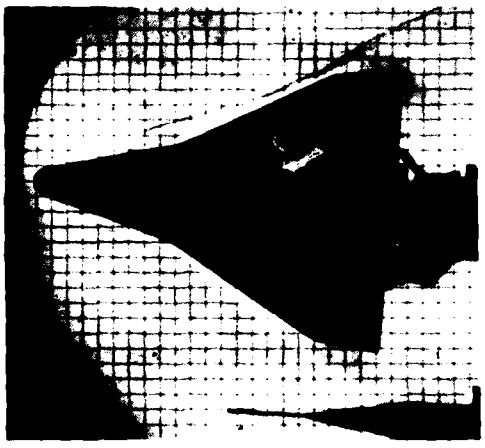

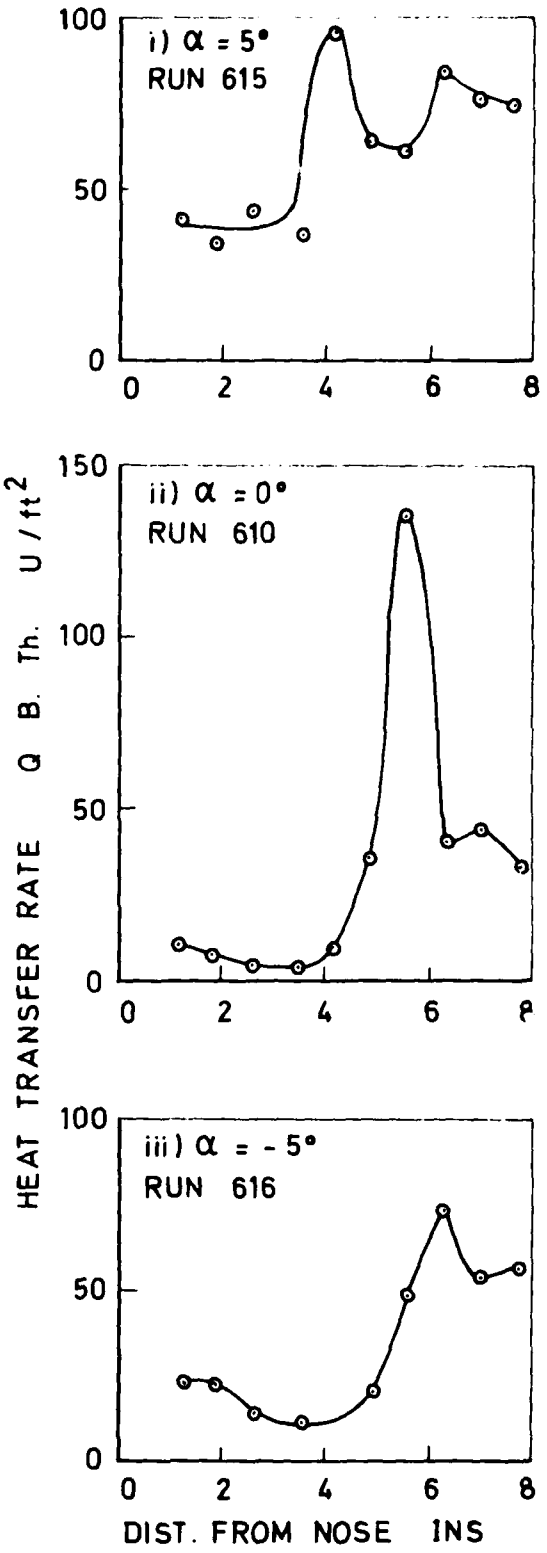

FIG 8a - SCHLIEREN PHOTOGRAPHS AND HEAT TRANSFER RATE.
M = 20, Re = 3.3×10^6 per ft. $-5° < \alpha < +5°$

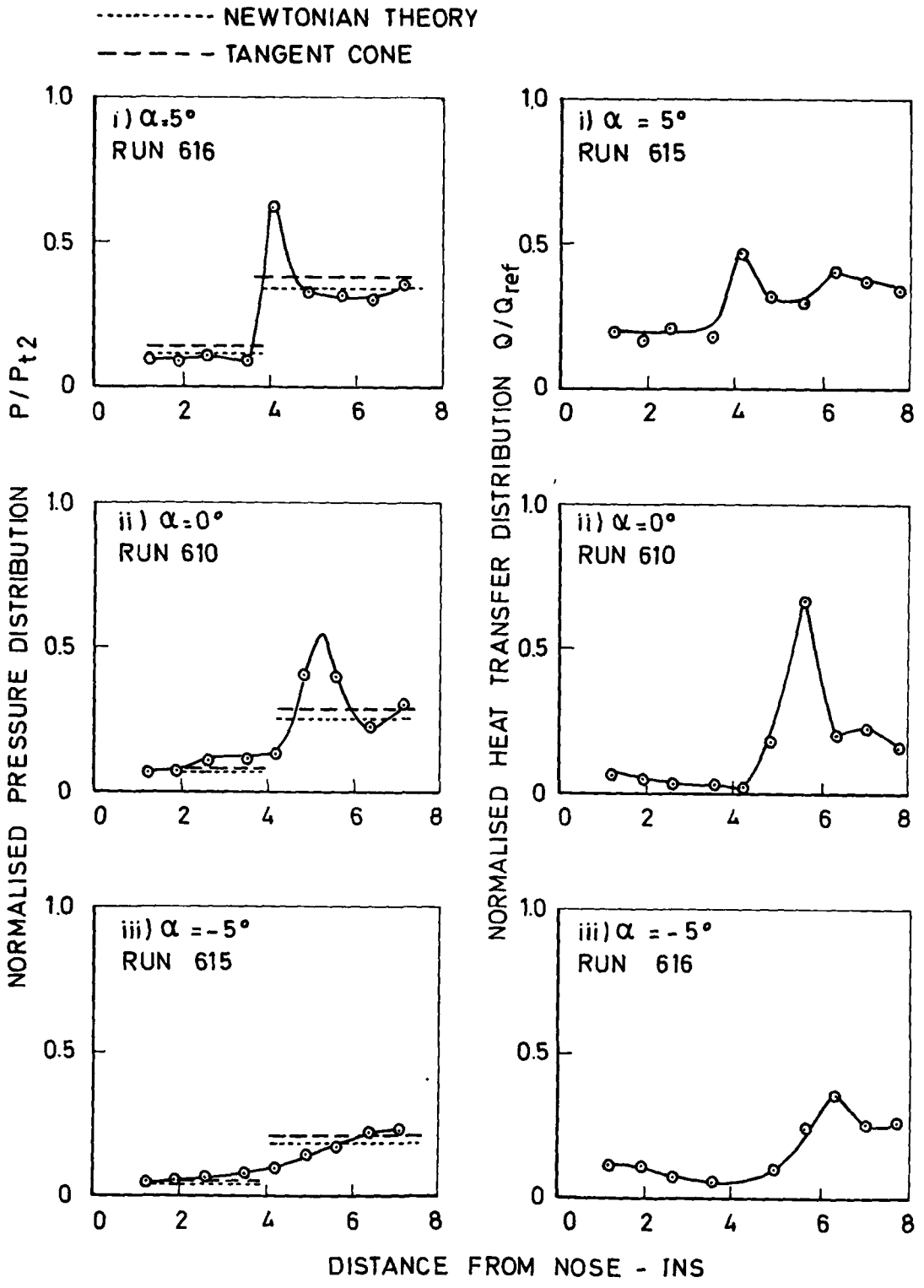

FIG. 8 b - NORMALISED PRESSURE AND HEAT TRANSFER DISTRIBUTION.

M = 20 Re = 3×10^6 per ft. $-5° < \alpha < 5°$

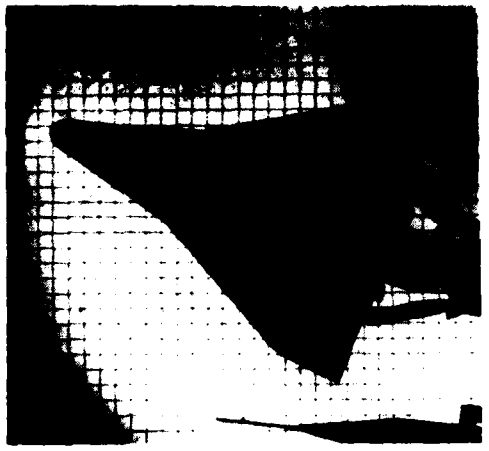

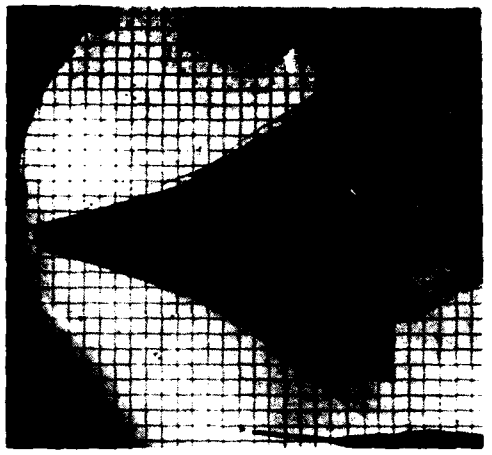

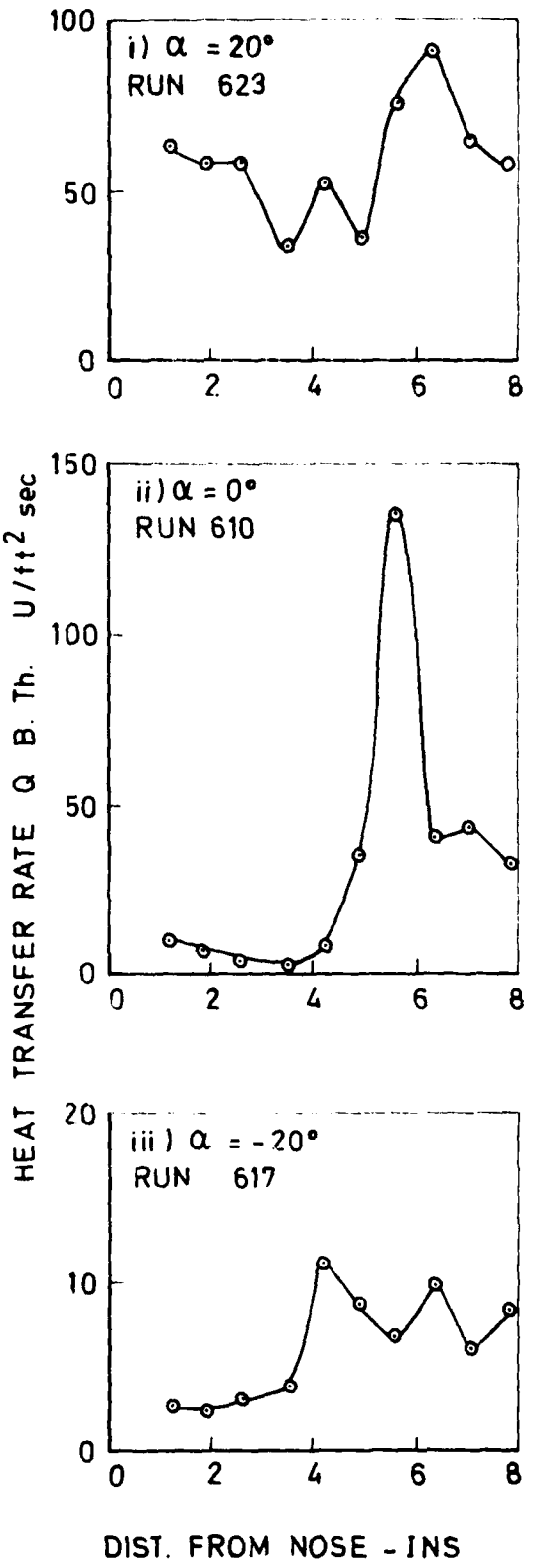

FIG. 9a SCHLIEREN PHOTOGRAPHS AND HEAT TRANSFER RATE

M = 20, Re = 3.3×10^6 per ft $-20° < \alpha < 20°$

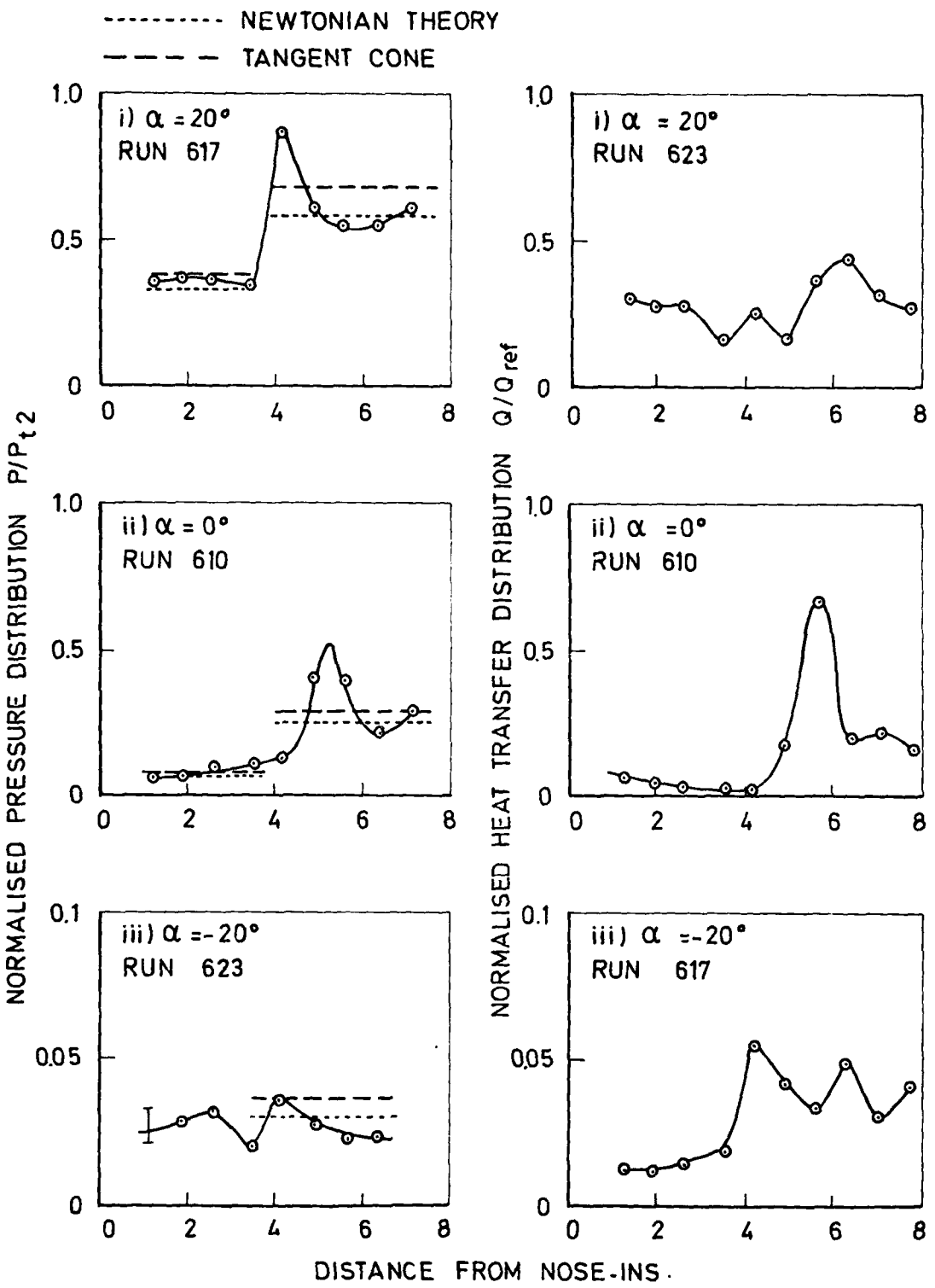

FIG. 9 b - NORMALISED PRESSURE AND HEAT TRANSFER RATE
M = 20 Re = 3.3×10^6 per ft. $-20° < 0 < 20°$

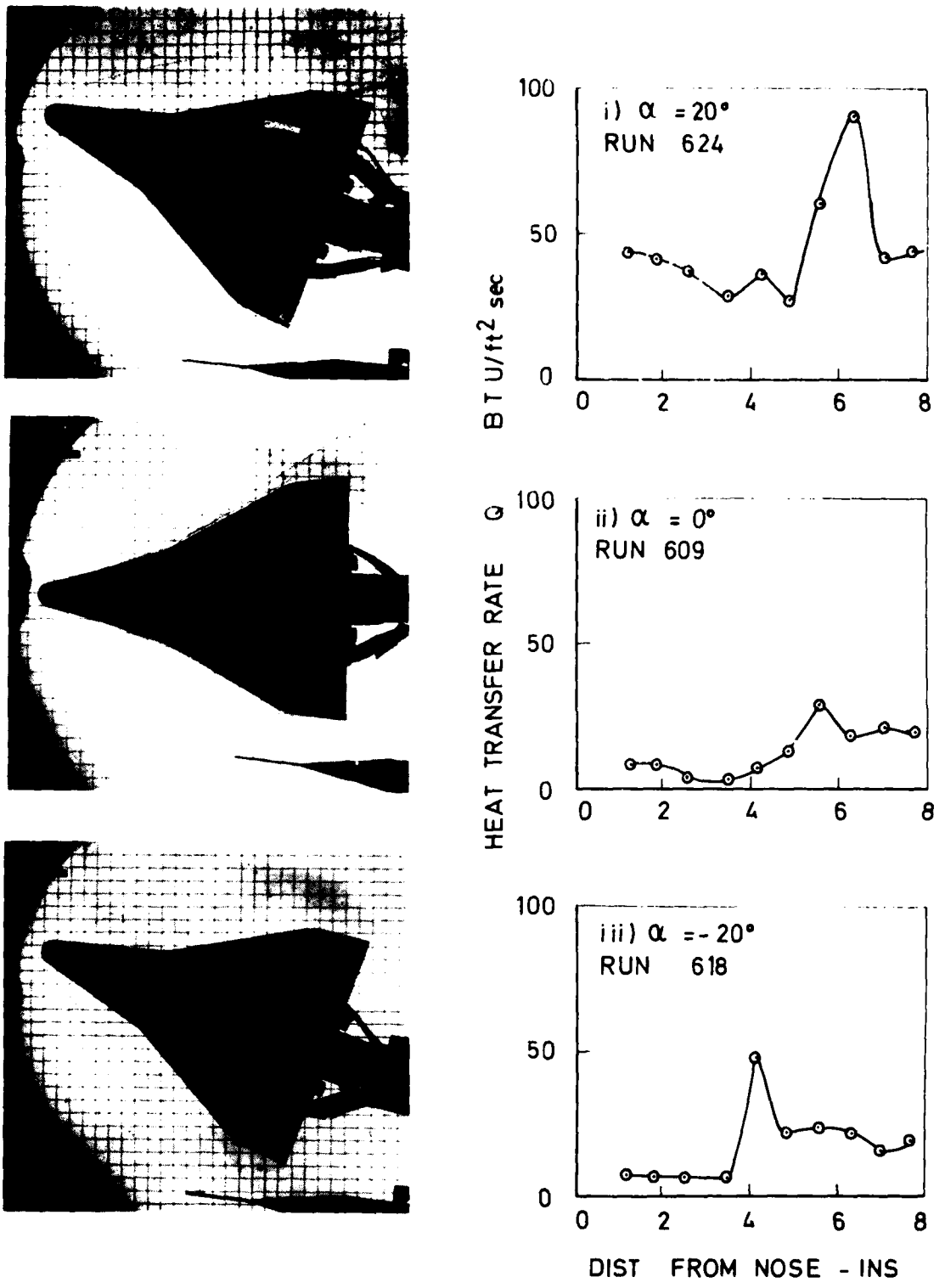

FIG 10a - SCHLIEREN PHOTOGRAPHS AND HEAT TRANSFER RATE

M = 20, Re = 2.0×10^6 per ft

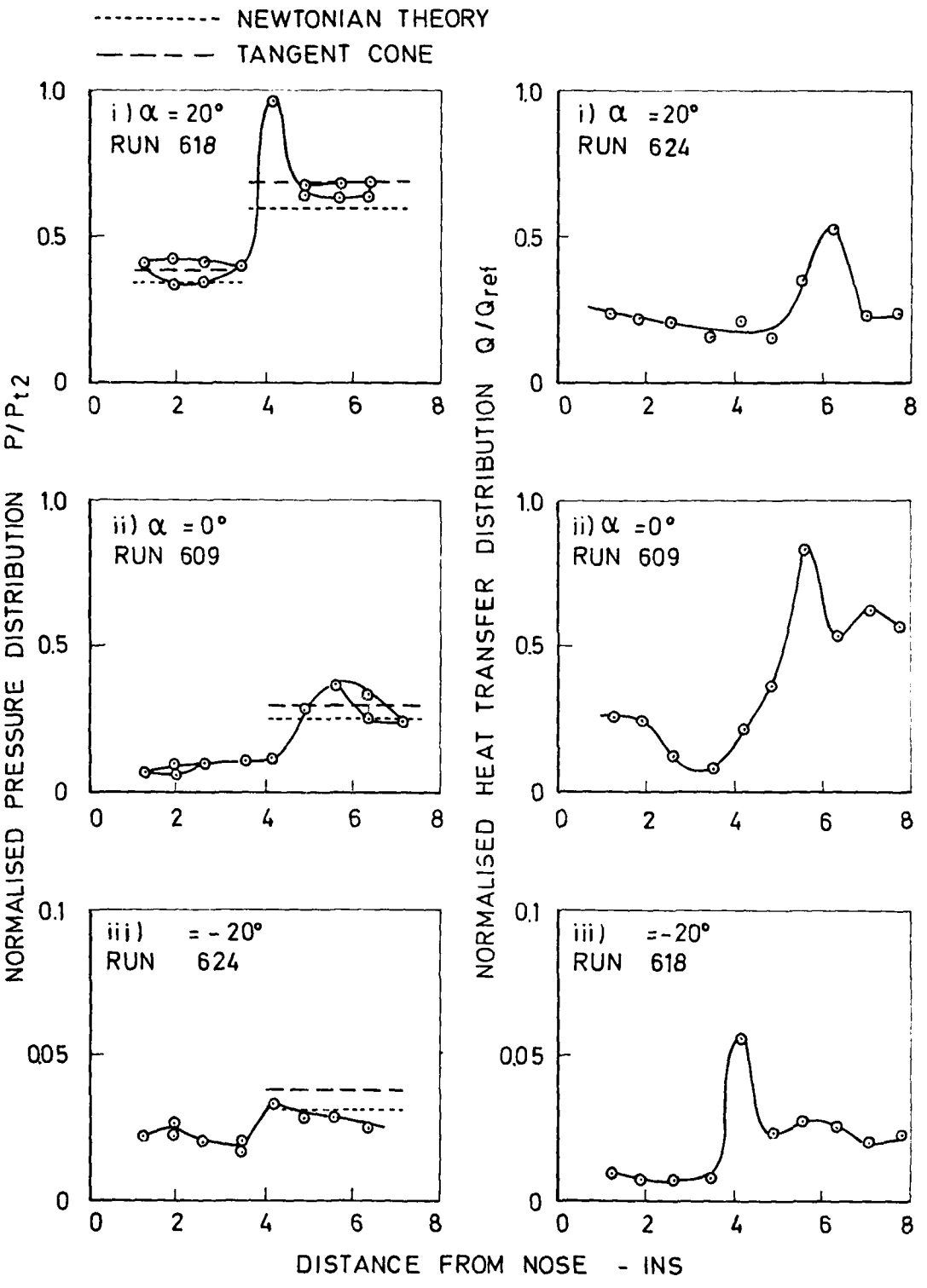

FIG.10 b-NORMALISED PRESSURE AND HEAT TRANSFER DISTRIBUTIONS

$M = 20$, $Re = 2 \times 10^6$ per ft. $-20° < \alpha < 20°$